ACOUSTIC NOISE SUPPRESSION: COMPROMISES IN IDENTIFICATION AND CONTROL

Ricardo S. Sánchez Peña, Miquel A. Cugueró, Albert Masip, Joseba Quevedo, Vicenç Puig
Sistemas Avanzados de Control, ESAII, Universidad Politécnica de Catalunya,
Rambla Sant Nebridi 10, Terrassa, Barcelona, España

Keywords: Active acoustic noise suppression, robust identification, $\mathcal{H}_\infty$ control, μ–analysis.

Abstract: The objective of this work is to explicitly point out the compromises in the identification and control stages in an acoustic noise suppression experiment, in terms of performance vs. controller order. The identification is a control–oriented robust procedure which takes into account both, parametric and non–parametric models, and is applied to the primary and secondary circuits of an acoustic tube. The control is designed via the $\mathcal{H}_\infty$ optimal control theory, and the analysis of the closed loop system is performed via the structured singular value (μ).

1 INTRODUCTION

Uncertainty in models which describe physical systems has deserved a great deal of attention. Robust Control and Identification techniques have worked with this hypothesis in the ’80s and ’90s respectively. Uncertainty has been considered both as unstructured (or global dynamic) and structured (either parametric or dynamic). Control design techniques are quite different in both cases. Parametric analysis and design is known to be an NP-hard problem (Braatz. et al., 1994; Puig et al., 2003). Instead for global or structured dynamic uncertainty optimal control methods can be used as the well known $\mathcal{H}_\infty$ control and μ–synthesis, respectively.

The area of Control oriented Identification seeks either a frequency domain or time domain unstructured uncertainty family of models from a deterministic worst case viewpoint (Chen and Gu, 2000), Chap 9 of (Sánchez Peña and Sznaier, 1998). Further research led to combinations of time and frequency domain measurements (Parrilo et al., 1998) as well as parametric and non–parametric models (Parrilo et al., 1999).

Here we will use some results from the Robust Identification area which combines parametric and dynamic models (Parrilo et al., 1999; Baldelli et al., 2001; Mazzaro et al., 2004) to obtain a global dynamic uncertain set describing the physical plant. In particular, interpolation results based on the general interpolation theory in (Ball et al., 1990) are applied, which potentially can combine both type of experimental data: frequency and time domain measurements (Parrilo et al., 1998).

The main objective of this work is to explicitly point out the compromises which arise in the identification and controller design stages of a particular problem. The application example is an acoustic noise suppression problem, which combines several characteristics of many other general problems: well defined parametric components, dynamic uncertainty, measurement noise, right half plane zeros feedforward and feedback control (Fang et al., 2004). This can be found in many other applications in the areas of civil, mechanical, aeronautics and aerospace engineering, e.g. active vibration suppression, robotics, large flexible structures, fluid instabilities in rocket motors, etc. Hence the results obtained in this case can be used elsewhere.

The main compromises which arise in this application are due to two well defined problems:

1. Right half plane zeros in the nominal model which limits the achievable performance see (Freudenberg and Looze, 1985) and an excellent survey in (Serón, 2005).
2. High relative modeling errors (multiplicative uncertainty) in frequencies where the experimental data is very small. This limits robust stability and as as a consequence, the achievable robust performance at these frequencies.

S. Sánchez Peña R., A. Cugueró M., Masip A., Quevedo J. and Puig V. (2005).
ACOUSTIC NOISE SUPPRESSION: COMPROMISES IN IDENTIFICATION AND CONTROL.
In *Proceedings of the Second International Conference on Informatics in Control, Automation and Robotics - Signal Processing, Systems Modeling and Control*, pages 251-257
DOI: 10.5220/0001172802510257

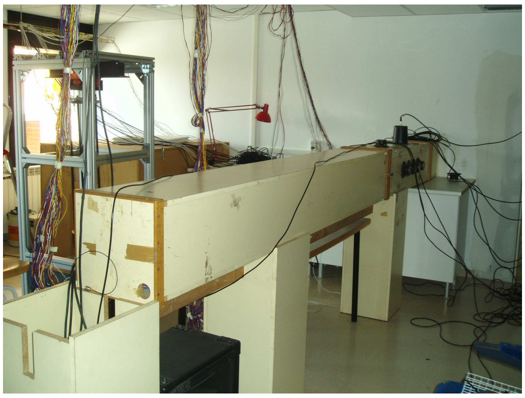

Figure 1: Acoustic tube connected to the anechoic room.

2 ACOUSTIC NOISE SUPPRESSION APPLICATION

The application is illustrated in figure 1. It consists of a 4 meter long square tube connected, in one side to an anechoic room and by the other to a noise generator through a primary speaker. It also contains a reference microphone near the noise generator and an error microphone near the control actuator (secondary speaker). The microphones are omnidirectional BEHRINGER ECM8000 with linear frequency response between 15 Hz and 20 kHz with -60 dB sensitivity. The speakers are BEYMA model 5 MP60/N of 5”, 50 W and frequency response between 50 Hz and 12 kHz.

The primary acoustic circuit goes from the reference to the error microphone. The secondary acoustic circuit is the one related to the feedback control section, that goes from the control speaker to the error microphone. Primary and secondary circuits are identified so that feedforward and/or feedback control can be applied, respectively. The controller is implemented with a DSpace DSP based on a Texas Instruments TMS320C0 over a DS1003.05 (Floating-Point Processor board).

The control scheme applies the classical method of generating a signal as close as possible to the real noise but with opposite phase. This can be performed in 2 ways, by feedforward and/or by feedback. In this work we will concentrate in this last approach, because the most interesting compromises arise in this case. Nevertheless a great deal of noise can be eliminated by combining both approaches, which will be explored in future works. Previous results in this application area can be found in (Fang et al., 2004) and its references. The authors have some previous experience in this area that has been presented in (Morcego and Cugueró, 2001; Masip et al., 2005). The conceptual setup is illustrated in figure 2 and its block diagram in figure 3.

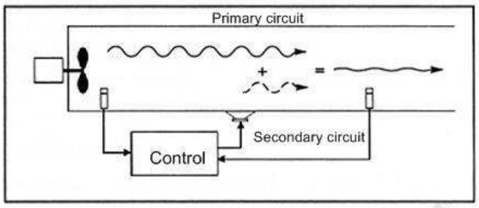

Figure 2: Conceptual view of acoustic noise suppression.

3 PARAMETRIC/DYNAMIC IDENTIFICATION

The identification procedure is based on (Parrilo et al., 1999; Baldelli et al., 2001), which combines parametric and dynamic models base on time and/or frequency experimental input data, and solved via LMI’s (Linear Matrix Inequalities) using the Toolbox in (Mazzaro et al., 2004). This in turn is based on a general rational interpolation theory developed in (Ball et al., 1990), which combines the classical frequency response (Nevanlinna-Pick) and time response (Carathéodory-Fejér) interpolation results.

Due to the fact that the model order in classical interpolatory results duplicates the number of data points (in the case of frequency data), it drastically reduces the model order to fit with parametric models (usually order 2) the most significant frequency peaks in the time and/or frequency response. Therefore, the remaining part of the plant can be suitably interpolated by a non–parametric dynamic model. This is valid not only in this application but in any other

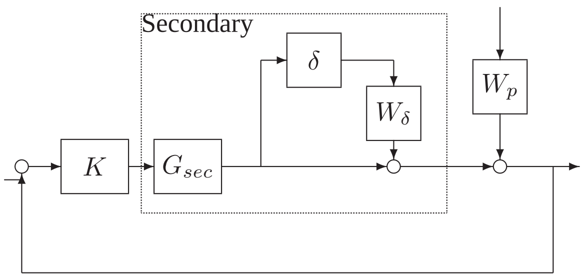

Figure 3: Feedback (FB) design setup, with primary circuit perturbation (W_p) and secondary model with multiplicative uncertainty.

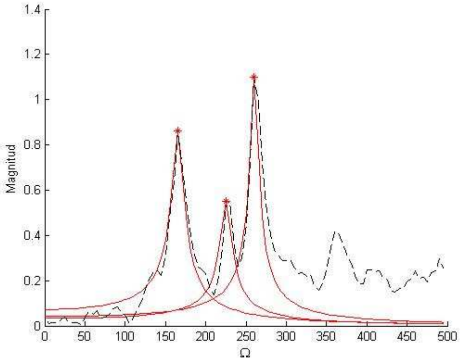

Figure 4: Kautz bases fitted to the secondary circuit data.

problem where well defined peaks are present in the experimental data, e.g. flexible structures.

The class of *a priori* plant and measurement noise models considered are in the framework presented in (Parrilo et al., 1998) and correspond to exponentially stable systems (finite or infinite dimensional) that satisfy the time domain bound

$$|h(k)| \leq K\rho^{-k}$$

with $K < \infty$ and $\rho > 1$. The experimental data are N_f (N_t) samples of the frequency (time) response of the system at frequency (time) values ω_k (t_k). The parametric information is fitted by means of a finite set of Kautz orthonormal basis $B_i(z)$ tuned to the experimental information as shown in (Baldelli et al., 2001). The resulting identified model has the form:

$$H_{id}(z) \quad = \quad H_{np}(z) + \sum_{i}^{N} p_i B_i(z), \quad p_i \in [a_i, b_i]$$

The optimization procedure which fits simultaneously the dynamic portion $H_{np}(z)$ and the parameters $\{p_i,\ i = 1, \ldots, N\}$ is solved via a set of LMI's, hence it is convex. Figure 4 illustrates the fitting of the Kautz bases to the experimental information. Note that only the first 3 peaks have been approximated by means of 2nd. order Kautz models, but not other peaks that raise at frequencies above 350 Hz. The reason will be explained in section 5 and has to do with the frequencies bands where performance is critical. In figures 5 and 12, the parametric and dynamic components and model error of primary and secondary acoustic circuits are presented, and in figures 6 and 7 the identified models.

From figures 5 and 12 it seems that the model error could be sufficiently small to provide a representative nominal model to design a controller. Nevertheless, the significance of this error varies according to the use we will make of it, as follows:

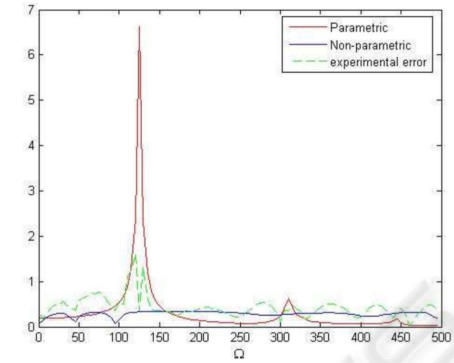

Figure 5: Parametric and dynamic models and model identification error of the primary circuit.

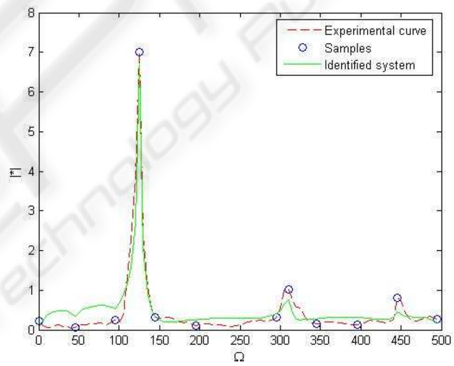

Figure 6: Identified model of the primary circuit.

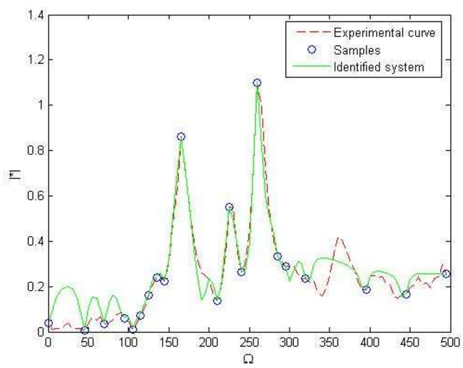

Figure 7: Identified model of the secondary circuit.

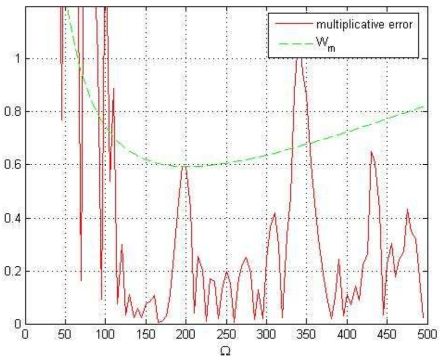

Figure 8: Uncertainty weight and multiplicative identification error.

Primary : The primary model can be used in 2 different ways.

- As a perturbation weight at the output for the controller feedback (FB) design. In this case only an approximation is enough, due to the fact that the objective of this weight is to emphasize the frequency bands where performance is required. In any case, the efficiency of the weight in recovering the important frequency bands will be verified at the robust performance analysis stage.
- As a model to be used in a feedforward (FF) or feedback/feedforward (FB/FF) scheme. Here the model is feeded with a signal that resembles the noise input to the actual primary circuit (as measured by the primary microfone) so that subtracting both output signals at the control speaker, the resulting acoustic noise will decrease. The efficiency of this procedure depends on the *additive* error of this model. Hence, the error depicted in figure 5 is the one to be considered, i.e. subtraction between model and experimental data.

Secondary : This model is used in the FB loop, and if the plant is represented by a multiplicative uncertainty set of models, the *relative* or *multiplicative* error is important, due to the fact that both, robust stability and performance depend on the value this error takes. Therefore, the error illustrated in figure 7 should be divided by the value of the experimental data (represented in figure 7), frequency by frequency. This can take very high values where the experimental data is near zero magnitude, as in $\omega \approx 100$ Hz in the same figure, for example[1]. The multiplicative error is represented in figure 8.

[1]It does not help to consider additive uncertainty, because the inverse of the nominal model still appears in the robust stability test, i.e. $\|W_{add}(z)G_{sec}^{-1}(z)T(z)\|_\infty = \|W_\delta(z)T(z)\|_\infty < 1$.

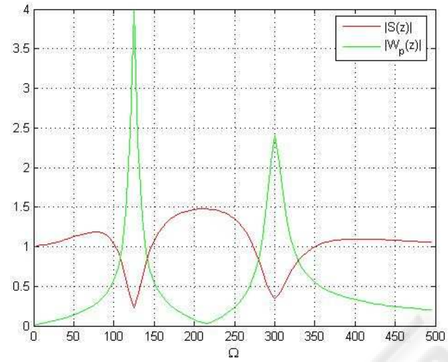

Figure 9: Sensitivity function and performance weight.

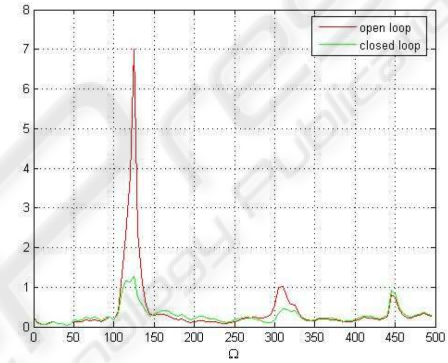

Figure 10: Open vs. closed loop comparison (first design).

4 ROBUST CONTROL

The control design procedure is the standard $\mathcal{H}_\infty$ optimal control technique applied to solve a mixed sensitivity problem. The objective is to minimize the effect in the output of the perturbation (acoustic noise) coming from the primary circuit (represented by $W_p(z)$) for all models described by the global dynamic (multiplicative) set $\mathcal{G} \triangleq \{[1 + W_\delta(z)\delta]\, G_{sec}(z)\}$. This can be seen from figure 3 and is a standard problem (Doyle et al., 1992) that can be solved suboptimally as follows:

$$\min_{K(z)} \left\| \begin{bmatrix} T(z)W_\delta(z) \\ S(z)W_p(z) \end{bmatrix} \right\|_\infty$$

In general, the optimal solution can be provided by μ–synthesis at the expense of a higher order controller. Nevertheless, in this case both solutions are coincident (Sánchez Peña and Sznaier, 1998; Zhou et al., 1996), due to the fact that the system is SISO.

It is clear from the above that the performance objective is to decrease the sensitivity to the signal provided by the primary circuit. In particular it is im-

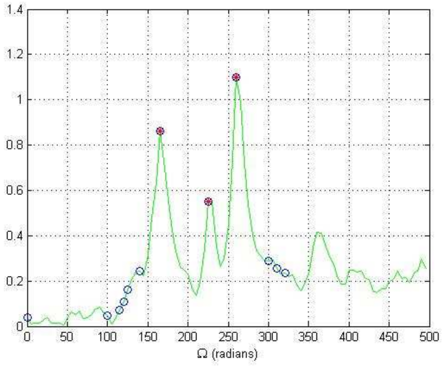

Figure 11: Less interpolation points concentrated in performance region, for secondary circuit to reduce order model.

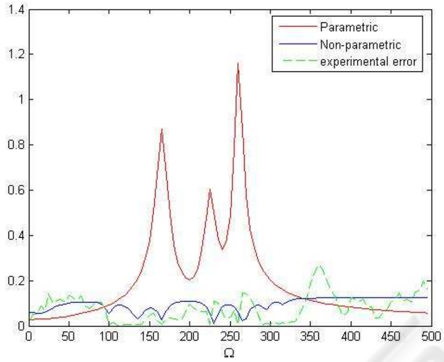

Figure 12: Parametric, dynamic and model error for secondary circuit (2nd design).

portant to achieve this at the peaks of the primary circuit's response. Therefore, $W_p(z)$ has been selected such that it increases the performance in frequencies where the primary acoustic circuit has a larger gain. As a consequence, the sensitivity attenuation will be greater at those peaks (see figure 9). On the other hand, $W_\delta(z)$ has been obtained from the multiplicative error as pointed out previously (see figure 8). Special care has been taken to reduce this error at frequencies where high performance is needed, as will be explained in the next section.

5 IDENTIFICATION AND DESIGN COMPROMISES

Besides maximizing performance and robustness, it is important to consider several practical constraints which should be taken into account. These, will therefore generate necessary compromises in the controller design and in possible identification iterations.

1. The nominal model of the (secondary) system is stable, but has right half plane zeros.
2. The multiplicative identification error is very difficult to decrease in frequency bands where the (secondary) system has a very small gain, e.g. $\omega \approx 100$ Hz.
3. The controller order should be kept as low as possible, due to the fact that it will be implemented with a DSP that has limited resources.

The solutions adopted for each of these issues are exposed next.

1. Non minimal phase models restrict performance in a well known way. In fact they suffer from the *waterbed* effect pointed out in (Freudenberg and Looze, 1985; Serón, 2005), which determines lower bounds in the size of the peaks of the sensitivity function $\|S(z)\|_\infty$. It is clear from here that the lower the sensitivity will be in certain bands, the higher it will increase in others. Hence, the performance weight W_p should reflect a decrease in the sensitivity **only** on those frequency bands with the higher peaks of the primary circuit, i.e. $\Delta\omega$ in $[100, 150]$ and $[275, 350]$ Hz. These frequency bands will be called "performance" bands. In this way, nominal performance should be achieved as follows: $\|W_p S\|_\infty < 1$.
2. The multiplicative identification error restricts not only robust stability, but also performance robustness. Therefore it should be decreased **only** in the regions where higher performance is needed, i.e. at the "performance" bands pointed out previously. This has been solved by adding more interpolation points in these frequency bands, while keeping the total number of points as low as possible not to increase the order, as will be seen next.
3. The controller order is equal to the order of the nominal model plus that of the weights W_p and W_δ. Therefore, the order of both weights have been kept as low as possible, while taking into account the performance and robustness features pointed out before:

$$W_p(s) = \prod_{i=1}^{2} \frac{k_i s}{s^2 + s\omega_{ni}\xi_i + \omega_{ni}^2} \quad (1)$$

$$W_\delta(s) = 6\frac{(s/200+1)^2}{(s/10+1)(s/1500+1)} \quad (2)$$

with $(k_1, \omega_{n1}, \xi_1) = (4, 125, 0.03)$ and $(k_2, \omega_{n2}, \xi_2) = (2.6, 300, 0.03)$. These continuous time weights have been transformed to discrete time by means of the classical bilinear transform with parameter $2/T_s$ where T_s is the sampling time. On the other hand, the order of the nominal model has been decreased by eliminating interpolation points and concentrating them in the important "performance" bands. In addition, higher frequency peaks that appear above 350 Hz in figure 4, have not been fitted with Kautz bases for the same reason. Furthermore, a balanced model order reduction step has been applied to the complete model. Here, the Hankel singular values of the discarded modes have a magnitude similar to measurement noise, so that the identification error is not increased.

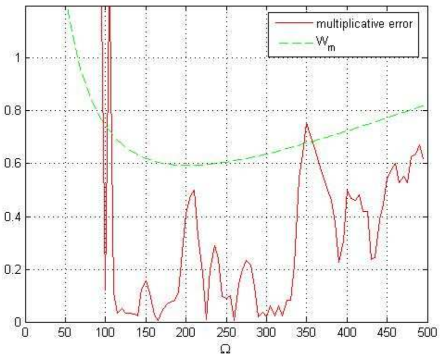

Figure 13: Uncertainty weight and multiplicative identification error (2nd design).

This requires a new identification iteration for the total design. Previously, 21 interpolating points and a 45th. order nominal model had been obtained (see figure 7). This in turn produced a 51st order controller which achieved a reduction in noise, at the two important frequency peaks of the primary circuit: 12.9dB for the first peak at $\omega = 125$ Hz and 6.8dB for the second peak at $\omega = 310$ Hz, as illustrated in figure 10.

Next, only 12 interpolation points are considered (figures 11 and 12) and a 25th order model is produced, which leads to a 31th. order robust controller. Note that in figure 12, the error is lower than in the previous case at the frequency bands $[100, 150]$ and $[275, 350]$ Hz. As a consequence, the multiplicative error is better in these "performance" regions, as illustrated in figure 13.

The controller produces a slightly worst noise reduction performance, but still near to the previous design, 12.5dB for the first peak and 6.17dB for the second one, as illustrated in figure 14. This reduction is at the expense of an amplification at other frequencies due to the *waterbed* effect, although at these other frequency bands the primary gain is negligible, as we have deliberately designed for. Compared with other works in this area (Fang et al., 2004), this is a reasonable result.

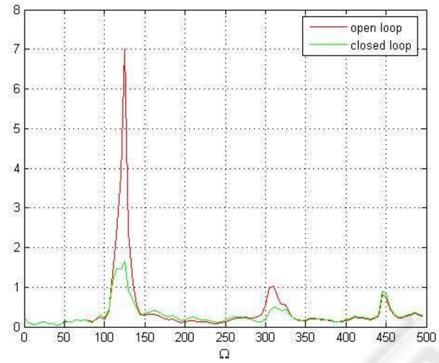

Figure 14: Open vs. closed loop comparison (second design).

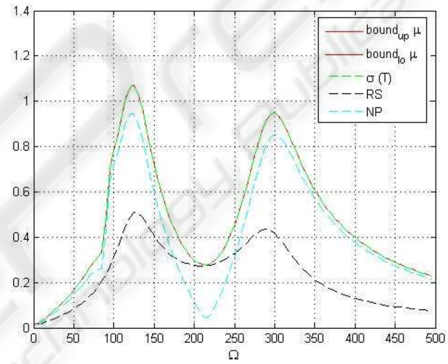

Figure 15: Structured singular value robust performance analysis.

The design analysis is presented in figures 15 and 16. In the first one, nominal performance, robust stability and the robust performance test

$$|T(z)W_\delta(z)| + |S(z)W_p(z)| < 1, \quad \forall z = e^{\jmath\Omega T_s} \qquad (3)$$

are compared with the optimal measure provided by the structured singular value μ. As indicated previously, due to the fact that the system is SISO, the latter coincides with the analysis measure provided by (3).

Nevertheless, as observed in figure 13, the weight does not cover completely the multiplicative error below 100Hz, nor the structured singular value μ is below one in figure 15. The uncertainty weight W_δ is used for the design stage, but the practical robust performance measure should be provided by the actual multiplicative error in figure 13 replaced in equation (3). This can be seen in figure 16, where although μ is above unity, the practical robust performance measure remains below 1, the reason being

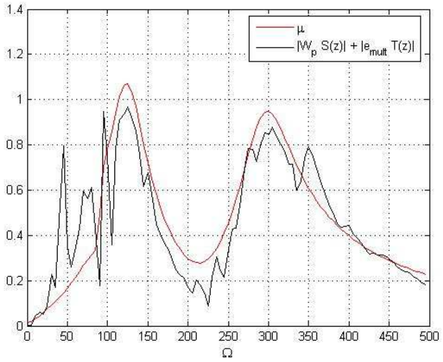

Figure 16: Practical robust performance analysis.

that in the frequency band where uncertainty is very high, a very low performance is required.

6 CONCLUSION

Here we have presented an example of a parametric/non–parametric identification and robust control technique applied to acoustic noise suppression in a tube. The main compromises, driven by practical issues, that limit the achievable performance have been discussed. The limitations imposed by non minimum phase zeros, controller model order and achievable identification relative error have been pointed out, and explicitly related to performance, robustness and frequency weighted interpolation.

The problem has been approached by general interpolation theory, $\mathcal{H}_\infty$ optimal control and μ–analysis, as identification, design and evaluation tools, respectively. These impose well known quantitative limitations on the achievable performance due to the minimum multiplicative uncertainty that can be practically reached by the identification procedure, at the expense of increasing the model order. Future work in this area should explore parametric worst case identification and robust design methods that could bypass this limitation to achieve a better performance and/or obtain a lower order controller. In addition, general feed-forward/feedback control structures will be explored as well as adaptive and/or time varying procedures.

ACKNOWLEDGMENTS

The authors wish to thank the support received by the Research Commission of the Generalitat of Catalunya (ref. 2001SGR00236) and by Spanish CICYT (ref. DPI2002-02147).

REFERENCES

Baldelli, D., Mazzaro, M. C., and Sánchez Peña, R. S. (2001). Robust identification of lightly damped flexible structures by means of orthonormal bases. *IEEE Transactions on Control Systems Technology*, 9(5).

Ball, J., Gohberg, I., and Rodman, L. (1990). *Interpolation of Rational Matrix Functions,Operator Theory: Advances and Applications*, volume 45. Birkhäuser.

Braatz., R. D., Young, P. M., Doyle, J. C., and Morari, M. (1994). Computational complexity of μ calculation. *IEEE Transactions on Automatic Control*, 39(5).

Chen, J. and Gu, G. (2000). *Control-Oriented System Identification - An $\mathcal{H}_\infty$ Approach*. Willey Inter-Science.

Doyle, J. C., Francis, B., and Tannembaum, A. (1992). *Feedback Control Theory*. Maxwell/Macmillan.

Fang, B., Kelkar, A., Joshi, S., and Pota, H. (2004). Modelling, system identification, and contrl of acoustic-structure dynamcs in 3D enclosures. *Control Engineering Practice*, 12:989–1004.

Freudenberg, J. and Looze, D. (1985). Right half plane poles and zeros and design tradeoffs in feedback systems. *IEEE Transactions on Automatic Control*, 30(6):555–565.

Masip, A., Puig, V., and Quevedo, J. (2005). An optimization based approach to interval model identification in the frequency domain. In *Proceedings IFAC, Prague*.

Mazzaro, M. C., Parrilo, P. A., and Sánchez Peña, R. S. (2004). Robust identification toolbox. *Latin American Applied Research*, 34(2):91–100.

Morcego, B. and Cugueró, M. (2001). Comparación de implementaciones en C y Matlab de filtros adaptativos para DSP. In *XXII Jornadas de Automática (UAB)*, Barcelona, Spain.

Parrilo, P. A., Sánchez Peña, R. S., and Sznaier, M. (1999). A parametric extension of mixed time/frequency robust identification. *IEEE Transactions on Automatic Control*, 44(2):364–369.

Parrilo, P. A., Sznaier, M., Sánchez Peña, R. S., and Inanc, T. (1998). Mixed time/frequency-domain based robust identification. *Automatica*, 34(11):1375–1389.

Puig, V., Saludes, J., and Quevedo, J. (2003). Worst-Case simulation of discrete linear Time-Invariant interval dynamic systems. *Reliable Computing Journal*, 9:251–290.

Sánchez Peña, R. S. and Sznaier, M. (1998). *Robust Systems Theory and Applications*. John Wiley & Sons, Inc.

Serón, M. M. (2005). Límites de desempeño y compromisos en sistemas de control. *Revista Iberoamericana de Automática e Informática Industrial*, 2(1):4–18.

Zhou, K., Doyle, J. C., and Glover, K. (1996). *Feedback Control Theory*. Prentice–Hall.